Journal of Applied Polymer Science

Fabrication of cellulose acetate ultrafiltration membrane with diphenyl ketone via thermally induced phase separation

Bo Pang,[1] Qian Li,[1] Yuanhui Tang,[2] Bo Zhou,[1] Tianyin Liu,[1] Yakai Lin,[1] Xiaolin Wang[1]

[1]Beijing Key Laboratory of Membrane Materials and Engineering, Department of Chemical Engineering, Tsinghua University, Beijing 100084, P. R. China

[2]School of Chemical & Environmental Engineering, China University of Mining & Technology, Beijing, Beijing 100083, China

Correspondence to: X. Wang (E-mail: xl-wang@tsinghua.edu.cn)

ABSTRACT: With diphenyl ketone as diluent, cellulose acetate (CA) ultrafiltration (UF) membrane with a bicontinuous structure was prepared via thermally induced phase separation (TIPS) method. The liquid–liquid phase separation region of CA/diphenyl ketone system was measured and the maximum corresponding polymer concentration was approximately 53 wt %. The effects of polymer concentration, coarsening time and coarsening temperature on the morphologies, and mechanical properties of CA membranes were investigated systematically. As the polymer concentration increased from 15 to 30 wt %, the bicontinuous structure could be obtained and the tensile strength of CA membranes increased from 3.92 to 30.17 MPa. With the increase of coarsening time, the thickness of dense skin layer and the asymmetry of cross-section reduced. However, excess coarsening rendered the membrane morphology evolved from a bicontinuous structure to a cellular structure. When the coarsening time was 5 min, the bicontinuous structure in cross-section showed good interconnectivity and the dense skin layer exhibited a thin thickness of 2 μm. The fabricated CA hollow fiber UF membrane exhibited a high tensile strength of 31.00 MPa and rejection of 96.10% for dextran 20 kDa. It is indicated that diphenyl ketone is a competitive diluent to prepare CA membranes with excellent performance via TIPS. © 2015 Wiley Periodicals, Inc. J. Appl. Polym. Sci. **2015**, *132*, 42669.

KEYWORDS: bicontinuous structure; cellulose acetate membrane; diphenyl ketone; thermally induced phase separation

Received 27 March 2015; accepted 26 June 2015

DOI: 10.1002/app.42669

INTRODUCTION

Currently, a high rate of population growth coupled with a rapid development of society bring about the global water crisis to be a realistic threat to the human being's survival and development.[1] As a novel chemical engineering unit operation, membrane separation technology has the advantages of wide separation scale, low cost, and friendly to environment.[2–4] Ultrafiltration (UF) has been widely used in the fields of wastewater treatment and pretreatment for an integral two-step microfiltration (MF) / UF - nanofiltration (NF) / reverse osmosis (RO) membrane operation.[5,6] Cellulose acetate (CA) is an important UF membrane material owing to its unique advantages of good hydrophilicity, antifouling property, abundant source, and biological degradation.[7] Furthermore, the existence of functional hydroxyl and ester groups in CA molecular structure renders CA membranes can be easily modified by a variety of methods, like grafting, surface coating, blending, etc.[7–10]

Nonsolvent-induced phase separation (NIPS) and thermally induced phase separation (TIPS) methods are often used to fabricate CA UF membranes. In the NIPS method, an abundant of solvents can be used and macrovoids tend to be obtained because of the fast interdiffusion between solvent and nonsolvent.[6] The presence of macrovoids is generally unfavorable for the mechanical strength and operation stability of CA membranes, especially for the self-supporting hollow fiber membranes.[11–15] Therefore, a CA UF membrane with macrovoid-free structure is of great interest.

TIPS is another promising method to prepare UF membranes which has the advantages of small probability of macrovoid formation and strong controllability.[16] A bicontinuous structure can be obtained via TIPS method to guarantee the good mechanical strength, high porosity, and minimized transmembrane mass transfer resistance.[17] For TIPS method, the properties of the diluent are critically important in determining the thermodynamic phase diagram, morphology, property, and performance of membrane. Generally, it is preferred to create a broad liquid–liquid (L-L) phase separation region in order to obtain a bicontinuous structure and good mechanical strength for CA membranes.[18,19] When the interaction between polymer and diluent becomes favorable, the L-L phase separation region will be shrunk or even

not occur. The traditional diluents used for CA membrane, including triethylene glycol (TEG),[20] tetraethylene glycol (TetraEG),[20] and dimethyl sulfone (DMSO2),[21] have good interaction with CA and the CA/diluents systems show the narrow L-L phase separation regions or solid–solid (S-S) phase separation region, which is unfavorable to obtain a bicontinuous structure. 2-Methyl-2,4-pentanediol (MPD) and 2-ethyl-1,3-hexanediol (EHD) were used as diluents to prepare CA membranes, respectively, and the CA/diluent systems have broad L-L phase separation regions.[22] However, the low boiling points of MPD ($T_b = 197.1$°C) and EHD ($T_b = 243.2$°C) caused a severe evaporation of diluents during membrane preparation. Hence, it is desirable to select a diluent which not only has a good stability but also can be used to obtain a broad L-L phase separation region.

Diphenyl ketone, also called benzophenone, is widely used in the fields of printing, cosmetic, plastic packaging, and food processing.[23] It has the advantages of high boiling point ($T_b = 304.5$°C), low toxicity, and recovery ability. In our preceding work, PVDF membranes with a bicontinuous cross-section structure have been prepared by using diphenyl ketone as diluent for the first time.[18] The L-L phase separation region of PVDF/diphenyl ketone system is about 30 wt % of polymer concentration. Moreover, diphenyl ketone can be recycled and reused by using simple extraction and distillation unit operations, and the eco-friendly production of PVDF membranes has been realized in the industrial scale-up stage.[24] Even though there are significant differences in the aspects of molecular structures and properties between CA and PVDF, it is attractive to select a universal diluent to obtain a bicontinuous structure via thermally induced L-L phase separation.[21] A universal diluent is favorable to broaden the application scopes of TIPS method.

In this work, diphenyl ketone was selected as the diluent to prepare a CA membrane with a bicontinuous structure via TIPS method. The phase diagram of CA/diphenyl ketone was plotted and analyzed. Effects of CA concentration, coarsening time, and coarsening temperature on the morphologies and mechanical properties of CA membranes were studied systematically. Besides, a CA hollow fiber UF membrane was prepared to investigate the ultrafiltration performance.

EXPERIMENTAL

Materials

Cellulose acetate (CA) (acetyl content of 39.8%) was purchased from Huibao Chemical (Beijing, China). Characterized by using gel permeation chromatography, the molecular weight (M_w) and polydispersity index (PDI) of CA are 34 kDa and 2.38, respectively. The CA powder was dried at 90°C under vacuum for 6 h before use. Diphenyl ketone was used as the diluent and purchased from Dalian Xueyuan Specialty Chemical. Dimethyl silicone, ethanol, n-hexane, isobutanol and dextran 20 kDa were purchased from Sinopharm Chemical Reagent. Dimethyl silicone was used as oil bath medium. Ethanol and n-hexane were used as extractants. Isobutanol was used in porosity measurement. Dextran 20 kDa was used to conduct filtration experiment. All reagents were analytical graded and used without further purification.

Phase Diagram

The CA/diphenyl ketone samples with different polymer concentrations ranging from 10 to 45 wt % were prepared like that described in our previous work.[18] The mixture was placed in a 15-ml standard ampoule. The standard ampoule was protected by an argon atmosphere, sealed to avoid the evaporation of diluent and then put into an oven at 180°C. Keeping for 12 h in oven, the homogeneous solution could be obtained. Then, the standard ampoule quenched into liquid nitrogen to get CA/diphenyl ketone samples. The samples were sliced in pieces and placed between a pair of microscope coverslips. To prevent the evaporation of diphenyl ketone, a Teflon film of 300 μm thickness with a circle opening was inserted between the two coverslips. The coverslips were heated on a hot stage (THMS 600, Linkam, UK) at 180°C and kept for 3 min, and then cooled to 25°C at a controlled rate of 10°C min^{-1}. An optical microscope (BX51, Olympus, Japan) was used to observe the dynamic process of droplet growth and determine the cloud points of CA/diphenyl ketone samples by the appearance of turbidity.

Based on the Flory-Huggins solution thermodynamics theory,[27] the theoretical binodal line can be calculated by using the following equations:

$$\ln(1-\varnothing)+(1-1/x)\varnothing+\chi_{12}\varnothing^2=\ln(1-\gamma\varnothing)+(1-1/x)\gamma\varnothing+\chi_{12}(\gamma\varnothing)^2 \quad (1)$$

$$\ln(\varnothing)+(1-x)(1-\varnothing)+\chi_{12}x(1-\varnothing)^2=\ln(\gamma\varnothing)+(1-x)(1-\gamma\varnothing)+\chi_{12}x(1-\gamma\varnothing)^2 \quad (2)$$

where $\varnothing$ represents the CA volume fraction in the polymer-rich phase, χ_{12} represents the interaction parameter between CA and diphenyl ketone, x represents the volume ratio of CA and diphenyl ketone molecules and γ represents the volume fraction ratio of CA in the polymer-rich phase and the polymer-poor phase.

The theoretical spinodal line can be calculated by using the following equation:

$$1/(1-\varnothing)-1+1/x-2\chi_{12}\varnothing=0 \quad (3)$$

The thermal properties of CA/diphenyl ketone mixture were determined like the method described in previous work.[25] Differential scanning calorimetry (DSC) measurement was conducted on TA instruments Q200. The samples of about 10 mg, sealed in a hermetical aluminum DSC pan, were heated and cooled under nitrogen atmosphere in the temperature range of 40–200°C. The heating and cooling rate were maintained at 10°C min^{-1}.

The crystallization behavior was characterized by an X-ray diffractometer (XRD, D8, BRUKER, Germany). The working electric current and voltage were set as 40 mA and 40 kV, respectively. The Cu : Ka radiation was employed on the samples. The scanning angle 2θ were from 5° to 60° with step size of 0.02° and time step of 0.1 s.

Membrane Preparation

In the case of membrane samples, the homogeneous CA/diphenyl ketone solution was obtained by the way described above and coated on the inner surface of the sealed ampoule.

Table I. The Experimental Conditions of CA Membrane Samples

Code	CA concentration (wt %)	Coarsening time (min)	Coarsening temperature (°C)
CM10	10	-	-
CM15	15	-	-
CM20	20	-	-
CM25	25	-	-
CM30	30	-	-
CM30-1-133	30	1	133.3
CM30-5-133	30	5	133.3
CM30-30-133	30	30	133.3
CM30-5-118	30	5	118.3

The ampoule quenched into ice water to get mixture samples. When coarsening was investigated, the ampoule was firstly immersed into oil bath and then quenched into ice water. The samples were extracted with ethanol and then conducted the solvent exchange with n-hexane to prevent the collapse of pores. Dry CA membrane was obtained after the volatilization of n-hexane. The thickness of CA membrane samples was about 400 μm. Effects of polymer concentration (10, 15, 20, 25, 30 wt %), coarsening time (1, 5, 30 min) and coarsening temperature (133.3, 118.3°C) were investigated, respectively. The experimental conditions for the preparation of CA membrane samples are listed in Table I.

In the case of hollow fiber membranes, a twin screw extruder was used as the fabrication apparatus. CA/diphenyl ketone mixture with CA concentration of 25 wt % was fed into the vessel. The hollow fibers were extruded from the spinneret, quenched into cooling bath, and wound by a take-up roller. Bore liquid was introduced to the inner orifice to make the lumen of hollow fibers. The cooling medium and bore liquid were water and glycerol, respectively. The temperatures of spinneret, cooling bath, and bore liquid were 170, 40, and 190°C, respectively. The dope flow rate was 16.7 g min^{-1}. The air gap between the spinneret and the water bath was 2 mm. The fibers were extracted with ethanol and then conducted solvent exchange with n-hexane. Dry CA hollow fiber membranes were obtained after the volatilization of n-hexane. Wet CA hollow fiber membranes were stored in a 50% aqueous glycerol solution.

Membrane Characterization

The dry CA membranes were fractured in liquid nitrogen and treated with platinum sputtering. The cross-section and surface structures of CA membranes were examined with a scanning electron microscope (SEM, JSM7401, JEOL, Japan).

The mean pore size (MPS) and pore size distribution (PSD) of the cross-section in the CA membrane sub-layer were observed directly by SEM and analyzed by Image-Pro Plus Version 6.0 software. The overall porosity of CA membrane samples were measured by gravimetric difference experiment. The completely dry CA membrane samples were weighed firstly, and then immersed in the isobutanol reagent for 12 h. The superficial adsorbed reagent was removed by filter paper carefully. Then, the weight of wet samples was measured quickly. The porosity of CA membranes, termed as A_k, can be calculated by the following equation:

$$A_k = \frac{(W_2 - W_1)/\rho_2}{W_1/\rho_1 + (W_2 - W_1)/\rho_2} \times 100\% \quad (4)$$

where ρ_1 and ρ_2 are the density of CA material and isobutanol, respectively. W_1 and W_2 are the weight of dry and wet CA membrane samples, respectively.

The tensile stress and strain test of the resulting CA membranes were measured by a tensile testing instrument (Z005, Zwick Roell, Germany). The membrane samples were prepared in rectangle shape with a length of 25 mm and a width of 5 mm. The thickness was around 400 μm and exactly measured by an electronic micrometer. The lengths of CA membrane samples and hollow fibers fixed between two pairs of tweezers were 15 and 50 mm, respectively. The test was conducted at the tensile speed of 5 mm min^{-1} under the condition of 20°C and a relative humidity of 20%. At least five parallel tests were carried out for each batch of CA membranes.

Ultrafiltration Experiment

The ultrafiltration experiments of CA hollow fiber membranes were conducted in a lab-scale filtration unit. The wet hollow fibers were removed from the aqueous glycerol solution and four fibers were assembled into a test module. Each fiber had an outer diameter of approximately 1.0 mm and effective length of 7.4 cm. The module was firstly rinsed with deionized water. The pure water or feed solution was pumped into the outer side of the fiber and the permeate solution was collected from the lumen side of the fiber. The membranes were firstly prepressured with de-ionized water at 6.0 bar for 3 h. Then, pure water flux was tested in depressurization procedure from 4.8 to 1.8 bar with an interval of 1.0 bar. Subsequently, the rejection experiment of dextran 20 kDa was conducted under 4.8 bar. The flow velocity was controlled at 60 L h^{-1} and the operation temperature was maintained 25°C. The concentration of dextran 20 kDa was 2000 ppm. The concentration of feed and permeate solutions was measured by a total organic carbon analyzer (TOC-V_{CPN}; Shimadzu, Japan). The flux (J_v, L m^{-2} h^{-1}) and rejection (R, %) were calculated by the following equations:

$$J_v = \frac{m}{\rho A \Delta t} \quad (5)$$

$$R = (1 - \frac{c_p}{c_f}) \times 100 \quad (6)$$

where m,ρ, A, Δt, c_p, c_f are the permeate mass (g), solution density (g L^{-1}), outside surface area of the membrane (m^2), time (h), concentration of dextran 20 kDa in the permeate and feed solutions, respectively.

RESULTS AND DISCUSSION

Phase Diagram

Figure 1 shows the thermodynamic phase diagram of CA/diphenyl ketone system, including a L-L phase separation region and a glass transition region. Cloud points were clearly observed during the cooling process for different polymer concentrations.

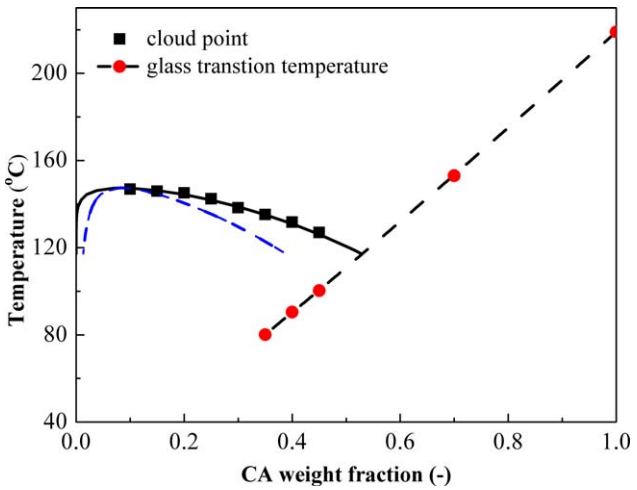

Figure 1. Phase diagram for the CA/diphenyl ketone system: (■) cloud points; (•) glass transition temperature. The black solid line and blue dash line represent theoretical binodal and spinodal lines, respectively. The black dash line represents the glass transition line. The glass transition temperature data of CA material was adopted from Ref. 28. [Color figure can be viewed in the online issue, which is available at wileyonlinelibrary.com.]

Theoretical binodal line and spinodal line were calculated and plotted, represented by the black solid line and blue dash line, respectively. The cloud points measured experimentally fit well with the binodal line. The L-L phase separation gap can be subdivided into a metastable region which is bounded between binodal and spinodal lines and an unstable region which is bounded by spinodal line. Nucleation and growth mechanism exists in the former region and spinodal decomposition mechanism exists in the latter region. The critical point, where binodal and spinodal lines coinside, is about 8 wt %. The intersection point of binodal line and glass transition line, also called Berghmans point, is approximately 53 wt % of the polymer concentration.

For CA/diphenyl ketone system, the solidification process is induced by the glass transition of CA. CA is a polymer with high glass transition temperature ($T_g = 219°C$).[28] The thermal signals of glass transition were detected by DSC measurement. As shown in Figures 1 and 2, the glass transition temperature decreased with the increase of diphenyl ketone content outside the L-L phase separation region. The temperature should remain constant inside the L-L phase separation region according to the phase rule. However, an obvious deviation from the horizontal line could be found which is probably because of the polydispersity of CA.

The microscope was used to observe the dynamic process of droplet growth during L-L phase separation and the results can be seen in Figure 3. For the CA/diphenyl ketone mixture with 20 wt % polymer concentration, when the homogeneous solution cooled from 180°C at the rate of 10°C min^{-1}, droplets began to appear at 145.1°C which corresponds to the cloud point of the system. As the temperature decreased, more and more droplets separated from homogeneous solution and the sizes of droplets increased gradually. The adjacent droplets contacted and coalesced. The growth of droplets was fast and obvious at the early stage of phase separation, while the growth rate decreased and it was difficult to observe the single droplet at the late stage of phase separation. As temperature decreased further, the L-L phase separation was arrested by the glass transition, accompanying with the sample changing from transparent to white opaque.

Figure 4 illustrates the XRD patterns of diphenyl ketone powder, CA(25 wt %)/diphenyl ketone (75 wt %) mixture with and without extraction. The sharp diffraction peaks presented in CA/diphenyl ketone mixture sample demonstrates the existence of crystallization. To determine the roles of CA and diphenyl ketone played in crystallization, XRD patterns of CA membrane sample and diphenyl ketone powder were detected. The diffraction peaks of diphenyl ketone powder matched well with those of CA/diphenyl ketone mixture sample while no diffraction peaks of CA could be found in CA membrane sample after the extraction of diphenyl ketone. Therefore, it can be reasonably inferred that even though CA is thought to be a semi-crystallized polymer,[29,31] CA was amorphous and glass transition induced the solidification in TIPS process.

Membrane Morphology

The composition of dope solution is one of the most important thermodynamic factors, which determines the initial position on the phase diagram and influences the membrane morphology. Usually, 10–30 wt % of polymer concentration is considered to be the reasonable scope in the preparation of UF membrane. Figure 5 shows the morphologies of CA membranes prepared with different polymer concentrations. Bicontinuous structure could be obtained in all range of polymer concentrations. When CA concentration was 10 wt %, the cross-section pores of CM10 tended to collapse. The cross-section morphologies of CM15–CM25 showed bicontinuous structures with good interconnectivity, while some isolated pores with decreased interconnectivity presented in CM30. Table II lists the mean pore size (MPS) and porosity of CA membranes. With the

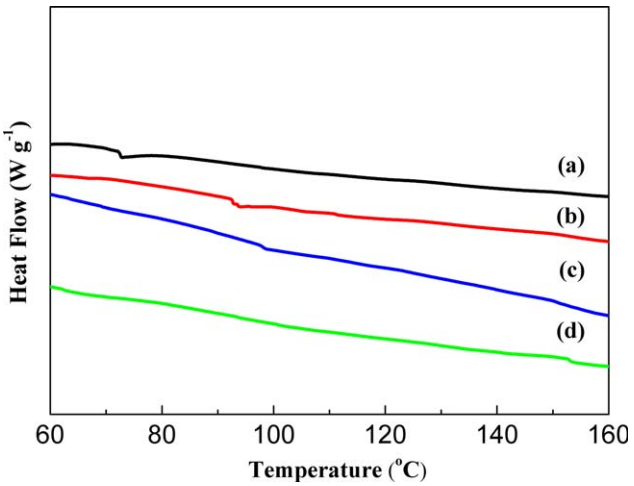

Figure 2. Glass transition temperature of CA/diphenyl ketone mixtures with different polymer concentrations: (a) 35 wt %, (b) 40 wt %, (c) 45 wt %, and (d) 70 wt %. [Color figure can be viewed in the online issue, which is available at wileyonlinelibrary.com.]

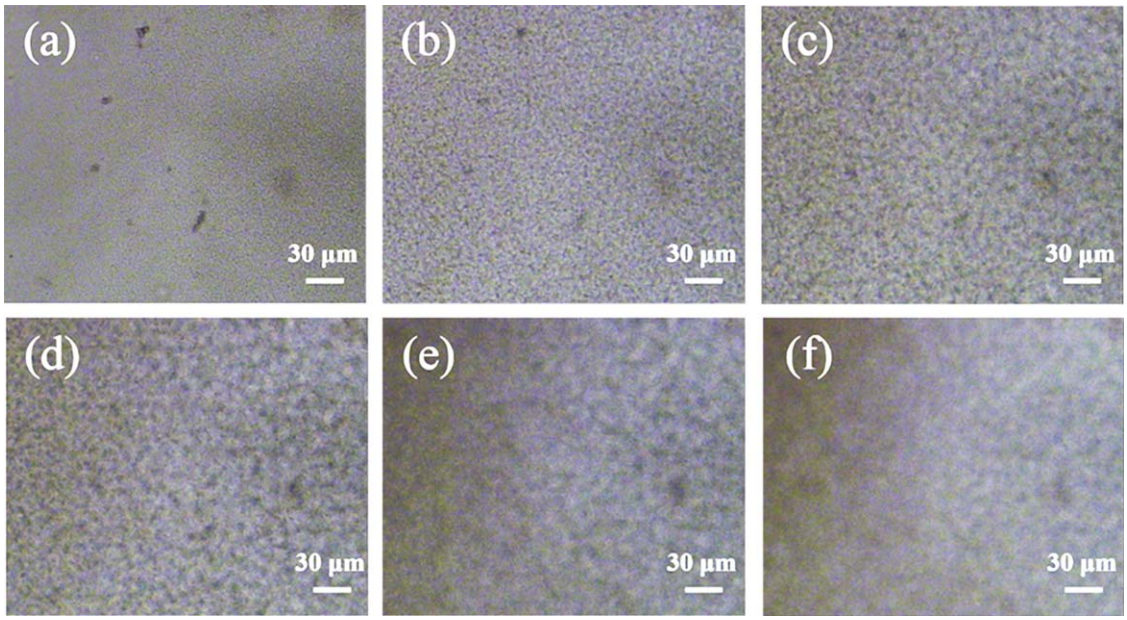

Figure 3. Optical images of droplet growth process in CA (20 wt %)/diphenyl ketone (80 wt %) mixture. The initial temperature of dope solution was 180°C and cooling proceeded at the rate of 10°C min^{-1}. The dope solution experienced (a) $T = 145.1$°C, (b) $T = 140.1$°C, (c) $T = 135.1$°C, (d) $T = 130.1$°C, (e) $T = 110.1$°C, and (f) $T = 90.1$°C. [Color figure can be viewed in the online issue, which is available at wileyonlinelibrary.com.]

increase of CA concentration from 15 to 30 wt %, MPS and porosity decreased from 0.37 μm and 73.3% to 0.19 μm and 52.5%, respectively. Figure 7(a) shows the pore size distribution (PSD) of the corresponding CA membranes. It can be found that with the increase of polymer concentration from 15 to 30 wt %, the peaks of PSD curves shifted to left side and the proportion of large size pores ($>$ 1 μm in diameter) decreased, which indicated that the MPS decreased and the pore uniformity increased. The change trends of MPS, porosity, and PSD are in agreement with SEM images (Figure 5).

As shown in the phase diagram (Figure 1), all of the compositions of dope solutions locate in the right side of critical point. It means that the polymer-lean phase forms the membrane pores and polymer-rich phase forms the membrane matrix. It has been demonstrated that the morphology of polymeric membrane prepared via L-L phase separation is influenced by the combination of spinodal decomposition and nucleation and growth mechanisms.[30] In this work, the quenching medium was ice water, and the quenching temperature was far below the cloud points and glass transition temperatures. L-L phase separation was dominated by spinodal decomposition mechanism and a bicontinuous structure could be obtained at the early stage of spinodal decomposition.[17] With the increase of polymer concentration, the viscosity of dope solution increases and the distance between cloud point and solidification point becomes closer (as shown in Figure 1). The increased viscosity and the shortened phase separation time are unfavorable to the growth of droplets during phase separation process, which leads to the decrease of MPS and porosity simultaneously.

Coarsening has been proven to be an effective means to improve membrane morphology.[32–34] Figure 6 shows the cross-section morphologies of CA membranes prepared in different coarsening conditions. Three coarsening times of 1, 5, and 30 min were investigated. As for the comparative sample, CM30 had an asymmetric cross-section structure with a dense skin layer of about 20 μm in thickness and a supporting porous network beneath the skin (Figure 6(a_2)). A short graded pore transition region existed along the membrane thickness and the MPS became uniform in the membrane sub-layer, shown in Figure 6(a_3, a_4). As for CM30-1-133, the asymmetric cross-section with a dense skin layer remained almost unchanged, shown in Figure 6(b_2). The MPS in the membrane sub-layer and the overall porosity slightly increased from 0.19 μm and 52.5% to 0.22 μm and 54.6%, respectively. When the coarsening time increased to 5 min, the cross-section morphology of CM30-5-133 changed obviously. From Figure 6(c_2–c_4), it can be found that the thickness of skin reduced significantly to about 2 μm and the graded pores structure could be obtained close to the

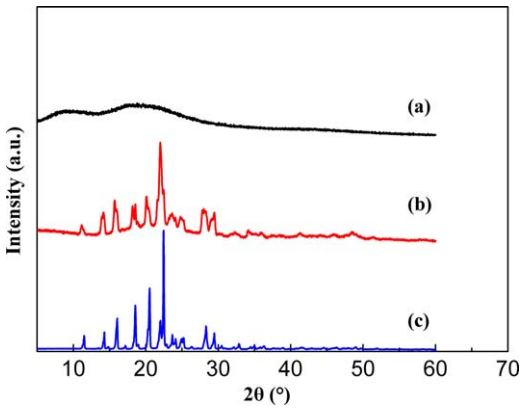

Figure 4. XRD patterns of (a) CM25, (b) CA (25 wt %)/diphenyl ketone (75 wt %) mixture sample, and (c) DPK powder. [Color figure can be viewed in the online issue, which is available at wileyonlinelibrary.com.]

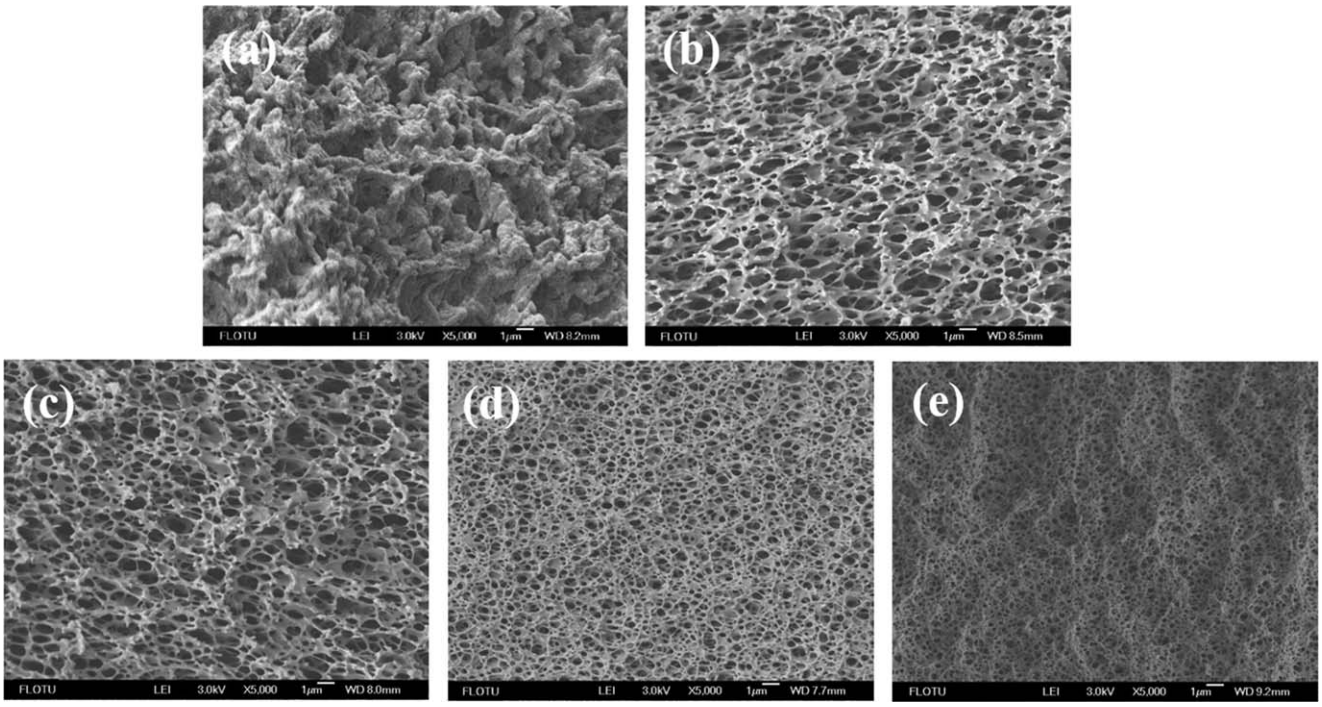

Figure 5. SEM images of the cross-section morphologies of CA membranes prepared with different CA concentrations: (a) CM10, (b) CM15, (c) CM20, (d) CM25, and (e) CM30.

skin. The uniform pore structure with improved interconnectivity and pore size existed in the membrane sub-layer. The MPS and porosity reached 0.34 μm and 61.5%. To further elongate the coarsening time to 30 min, the cross-section morphology of CM30-30-133 appeared to be symmetric and cellular pores with undesired interconnectivity could be found throughout. The MPS increased to 0.82 μm while the porosity decreased to 45.3%. As shown in Figure 7(b), with the increase of coarsening time, the peaks of PSD curves shifted to right side and the proportion of large size pores ($>$ 1 μm in diameter) increased, which indicated that the MPS increased and the pore uniformity decreased. The experimental observation is in agreement with the calculation results on the dynamics of membrane structure formation conducted by McHugh's group.[36,37] They found that when the phase separation temperature was above glass transition, the initial bicontinuous structure would undergo a percolation-to-cluster transition and the pore sizes gradients would gradually diminish with time.

Coarsening temperature, 133.3°C, locates between the binodal and spinodal lines which means that the dope solution was metastable and L-L phase separation was induced by nucleation and growth mechanism. A nucleus needs enough energy to reach the critical size before it becomes stable and begins to grow.[34] Coarsening process provides driving force to overcome the energy barrier for the formation and growth of droplets. Meanwhile, the coalescence of droplets results in the increase of pore size and the decrease of pore number.[35] When the coarsening time arrived at 5 min, an ideal bicontinuous cross-section structure with improved interconnectivity could be obtained. The further increase of coarsening time brought about the polymer-rich phase and the polymer-lean phase evolved from a bicontinuous structure to a sea-island structure, reflecting in the deterioration of interconnectivity of the final membrane pores.

Figure 6(e) illustrates the cross-section morphology of CM30-5-118 which prepared with coarsening temperature of 118.3°C for 5 min. The cellular structure of CM30-5-118 substituted the bicontinuous structure of CM30-5-133 [Figure 6(c)]. The MPS increased from 0.34 to 0.73 μm while the porosity decreased from 61.5% to 54.0%.

The coarsening temperature influences the phase separation mechanism and membrane morphology. Different from 133.3°C, the coarsening temperature of 118.3°C locates under the spinodal line, which means the dope solution is unstable and the L-L phase separation is induced by spinodal decomposition mechanism. With the decrease of coarsening temperature, the growth and coalescence of droplets are intensified at the late stage of spinodal decomposition. The presence of cellular pores was probably because of the effect of vigorous coarsening that

Table II. MPS and Porosity of Various CA Membrane Samples

Code	Thickness (μm)	MPS (μm)	Porosity (%)
CM15	367	0.37	73.3
CM20	420	0.32	68.4
CM25	444	0.24	64.0
CM30	377	0.19	52.5
CM30-1-133	400	0.22	54.6
CM30-5-133	448	0.34	61.5
CM30-30-133	414	0.82	45.3
CM30-5-118	322	0.73	54.0

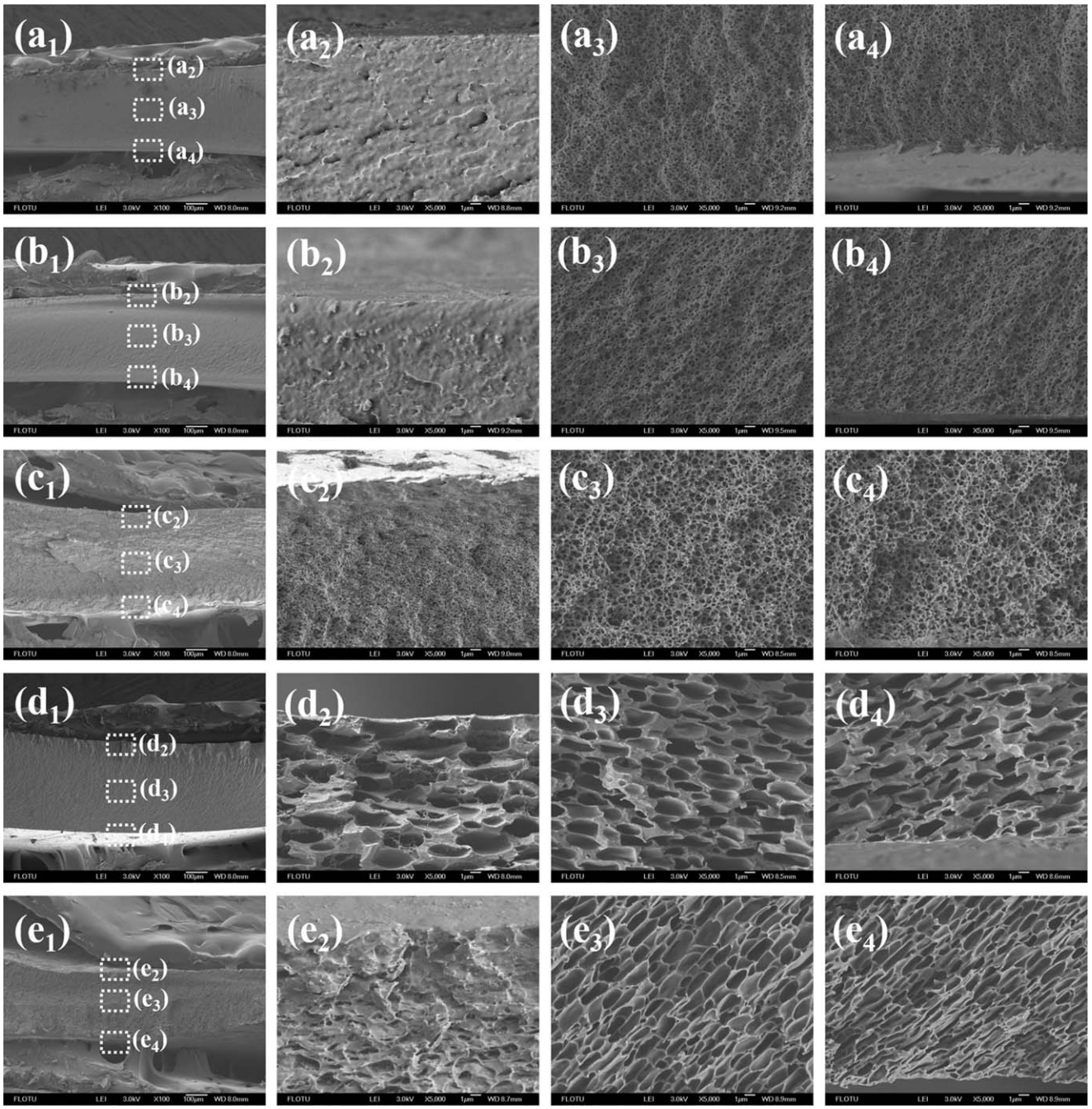

Figure 6. SEM images of the cross-section morphologies of CA membranes prepared in different coarsening conditions. The symbols a, b, c, d, and e represent CM30, CM30-1-133, CM30-5-133, CM30-30-133, and CM30-5-118, respectively. The subscript 1 represents the overall cross-section of ×100 magnification, and 2 represents the cross-section close to the upper surface of ×5000 magnification, and 3 represents the cross-section in the middle section of ×5000 magnification, and 4 represents the cross-section close to the bottom surface of ×5000 magnification.

rendered the polymer-rich phase and polymer-lean phase evolved from a bicontinuous structure to a sea-island structure.

Considering the results discussed above, it can be demonstrated that a bicontinuous structure can be obtained in the early stage of spinodal decomposition by rapid quenching. Coarsening process plays a critically important role in the later stages of phase separation induced by spinodal decomposition and nucleation and growth. The optimized cross-section morphology with improved interconnectivity and reduced skin thickness could be obtained for CM30-5-133.

Mechanical Strength

The mechanical strength is closely related to the membrane structure. As discussed above, the narrower PSD and the smaller MPS could be obtained in the cases of high polymer concentration, short coarsening time, and high coarsening temperature, which are favorable to the mechanical strength. Figure 8

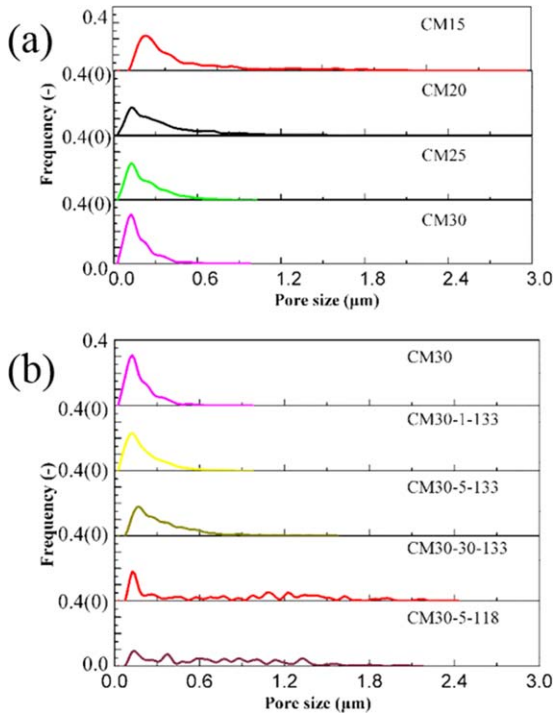

Figure 7. PSDs of CA membranes prepared with (a) different polymer concentrations and (b) different coarsening conditions. [Color figure can be viewed in the online issue, which is available at wileyonlinelibrary.com.]

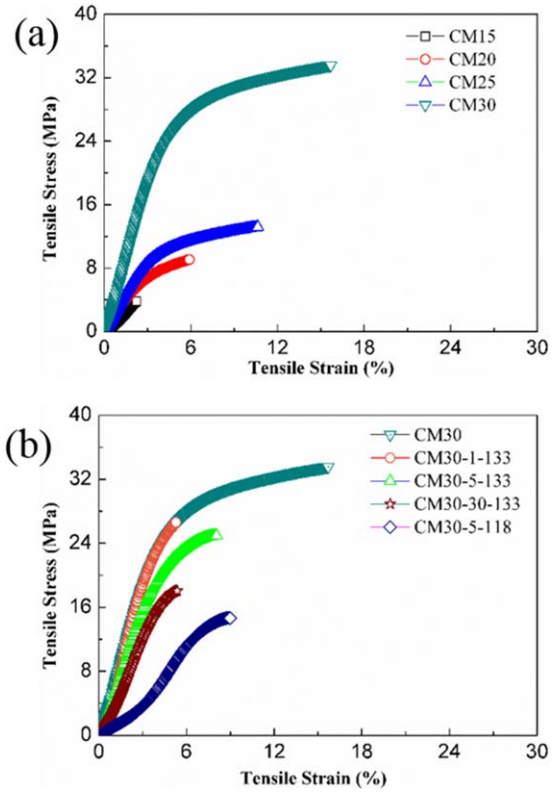

Figure 8. Tensile stress–strain curves of CA membranes prepared with (a) different polymer concentrations and (b) different coarsening conditions. [Color figure can be viewed in the online issue, which is available at wileyonlinelibrary.com.]

illustrates the tensile stress and strain of CA membranes prepared with different polymer concentrations and coarsening conditions. Initially, the tensile stress exhibited an approximately linear increase with the tensile strain. After the elastic deformation region, the yielding point was arrived and the plastic deformation resulted in the irreversible deformation of CA membranes. At the maximum stress point, the test samples failed by tearing sharply. As listed in Table III, the tensile strength increased from 3.92 to 30.17 MPa and elongation increased from 1.95% to 14.33% as the CA concentration increased from 15 to 30 wt % (CM15–CM30). Therefore, both the strength and toughness of CA membranes enhanced with the increase of CA concentration. Coarsening brought about the decrease of tensile strength and elongation. The mechanical strength of CA membranes prepared in different coarsening conditions located in the range of 14.55–26.45 MPa. The mechanical property in this work is better than that of the CA membranes (2.0−4.0 MPa of tensile strength) prepared via NIPS method, which can be attributed to the presence of interconnected pores and the absence of macrovoids in the membrane cross-section.[13,14,28,38–40] The excellent mechanical property is promising for CA membrane to be used in the UF process.

Ultrafiltration Performance

To date, few works were devoted to the preparation of CA hollow fiber membranes via TIPS process.[20,26] In this work, CA hollow fiber UF membranes were prepared by using CA/diphenyl ketone system. CA concentration is one of the most influential factors in determining the spinnability, self-supporting ability, and surface morphology of hollow fiber membrane.[41,42] 25 wt % of CA concentration was used to prepare hollow fiber membranes. The morphologies of the synthesized CA hollow fiber membranes are shown in Figure 9. The outside and inside diameters were about 1.00 and 0.52 mm, respectively. A bicontinuous cross-section structure and obvious asymmetry with the decreased pore size from lumen side to outer side could be observed. Meanwhile, a porous inner surface and a dense outer surface were formed. The asymmetry of cross-section structure was the result of concentration and temperature gradients. On one hand, the evaporation of diluent near the outer surface resulted in the concentration gradient across membrane thickness when a certain distance of air gap

Table III. Mechanical Properties of Various CA Membrane Samples

Code	Tensile strength (MPa)	Elongation (%)
CM15	3.92 ± 0.13	1.95 ± 0.35
CM20	8.94 ± 0.16	6.18 ± 0.38
CM25	12.70 ± 0.71	10.50 ± 0.71
CM30	30.17 ± 3.04	14.33 ± 2.08
CM30-1-133	26.45 ± 0.21	5.55 ± 0.35
CM30-5-133	23.00 ± 2.83	6.95 ± 1.34
CM30-30-133	17.65 ± 0.64	5.25 ± 0.07
CM30-5-118	14.55 ± 0.21	7.90 ± 1.41

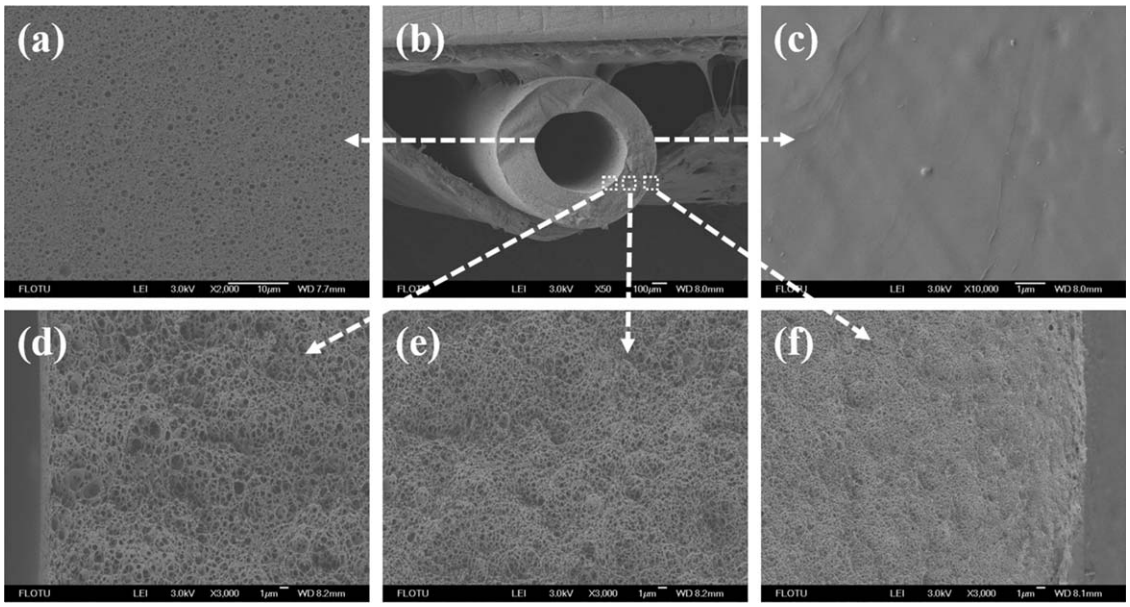

Figure 9. SEM images of the cross-section and surface morphologies of CA hollow fiber membrane. (a) Inner surface of ×2000 magnification, (b) overall cross-section of ×50 magnification, (c) outer surface of ×10,000 magnification, (d) cross-section close to inner surface of ×3000 magnification, (e) middle cross-section of ×3000 magnification, (f) cross-section close to outer surface of ×3000 magnification. The polymer concentration was 25 wt %.

existed. On the other hand, the temperature of bore liquid was much higher than that of external coagulant medium. When the fiber immersed into coagulant, the dope solution near the outer surface experienced phase separation and solidification at the faster speed, while the dope solution near the inner surface could coarsen for a relatively long time which facilitated the increase of pore size.

The property and performance of CA hollow fiber membrane are shown in Figure 10 and Table IV. The pure water flux increases linearly with the increase of operation pressure and pure water permeability obtained by fitting curve was 0.13 L m^{-2} h^{-1} bar^{-1}. The rejection of dextran 20 kDa arrived 96.1% and flux was about 1.15 L m^{-2} h^{-1} at 4.8 bar. It can be inferred that the molecular weight cut off (MWCO) of the CA hollow fiber membrane is below 20,000 Da. The tensile strength and elongation were 31.00 MPa and 30.80%, respectively. Therefore, a CA UF hollow fiber membrane with high mechanical strength and rejection performance can be prepared via TIPS method.

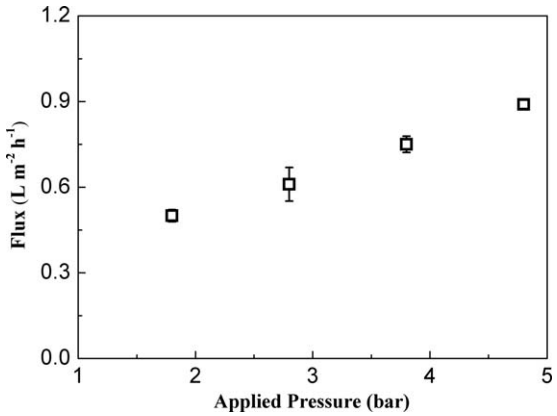

Figure 10. Pure water flux of CA hollow fiber membranes at different operation pressures.

CONCLUSIONS

In this work, cellulose acetate (CA) membrane with a bicontinuous structure was prepared via TIPS method with diphenyl ketone as diluent. The phase diagram of CA/diphenyl ketone showed a broad liquid–liquid phase separation region and the Berghmans point reached a high polymer concentration of approximate 53 wt %. As the polymer concentration increased from 15 to 30 wt %, the bicontinuous structure with the decreased mean pore size and porosity could be obtained, and the mechanical strength of CA membranes increased from 3.92 to 30.17 MPa. Coarsening process played a critically important role in controlling the membrane morphology. In the optimized condition of coarsening for 5 min at coarsening temperature of 133.3°C, the cross-section with improved porosity and reduced skin thickness could be obtained. The fabricated CA hollow fiber membranes showed the mechanical strength of 31.00 MPa and the rejection of dextran 20 kDa reached more than 95%. It

Table IV. Properties and Performance of CA HOLLOW FIBER MEMBRANES

Mechanical properties		Filtration performance		
Tensile strength (MPa)	Elongation (%)	Pure water permeability (L m^{-2} h^{-1} bar^{-1})	Flux (L m^{-2} h^{-1})[a]	Rejection (%)[a]
31.00	30.80	0.13	1.15	96.10

[a] Rejection experiment of dextran 20 kDa, the concentration of solute was 2000 ppm and operation pressure was 4.8 bar.

is believed that diphenyl ketone is a competitive diluent to prepare CA membranes with a bicontinuous cross-section structure and excellent mechanical property via TIPS. In the future work, the control of surface morphology of CA hollow fiber membranes will be investigated. It is attractive and promising to obtain the tunable selectivity for CA hollow fiber membranes prepared via TIPS method.

ACKNOWLEDGMENTS

The authors would like to thank National Key Technologies R&D Program of China (No. 2015BAE06B00), Tsinghua University Initiative Scientific Research Program (20121088039) and Natural Science Foundation of China (No. 20141300604) for providing the financial support in this work.

REFERENCES

1. Van der Bruggen, B.; Borghgraef, K.; Vinckier, C. *Water Resour. Manag.* **2010**, *24*, 1885.
2. Van Der Bruggen, B.; Vandecasteele, C.; Van Gestel, T.; Doyen, W.; Leysen, R. *Environ. Prog.* **2003**, *22*, 46.
3. Greenlee, L. F.; Lawler, D. F.; Freeman, B. D.; Marrot, B.; Moulin, P. *Water Res.* **2009**, *43*, 2317.
4. Pendergast, M. M.; Hoek, E. M. V. *Energy Environ. Sci.* **2011**, *4*, 1946.
5. Abetz, V.; Brinkmann, T.; Dijkstra, M.; Ebert, K.; Fritsch, D.; Ohlrogge, K.; Paul, D.; Peinemann, K. V.; Nunes, S. P.; Scharnagl, N.; Schossig, M. *Adv. Eng. Mater.* **2006**, *8*, 328.
6. Guillen, G. R.; Pan, Y. J.; Li, M. H.; Hoek, E. M. V. *Ind. Eng. Chem. Res.* **2011**, *50*, 3798.
7. Maheswari, P.; Barghava, P.; Mohan, D. *J. Polym. Res.* **2013**, *20*, 1.
8. Malaisamy, R.; Mahendran, R.; Mohan, D.; Rajendran, M.; Mohan, V. *J. Appl. Polym. Sci.* **2002**, *86*, 1749.
9. Kumari, A.; Sarkhel, G.; Choudhury, A. *J. Appl. Polym. Sci.* **2012**, *124*, E300.
10. Huang, C.; Tsai, C. Y.; Juang, R. S.; Kao, H. C. *J. Appl. Polym. Sci.* **2010**, *118*, 3227.
11. Saljoughi, E.; Amirilargani, M.; Mohammadi, T. *J. Appl. Polym. Sci.* **2009**, *111*, 2537.
12. Qin, J. J.; Li, Y.; Lee, L. S.; Lee, H. *J. Membr. Sci.* **2003**, *218*, 173.
13. Senthilkumar, S.; Rajesh, S.; Mohan, D.; Soundararajan, P. *Sep. Sci. Technol.* **2013**, *48*, 66.
14. Han, B. X.; Zhang, D. L.; Shao, Z. Q.; Kong, L. L.; Lv, S. Y. *Desalination* **2013**, *311*, 80.
15. Lv, C. L.; Su, Y. L.; Wang, Y. Q.; Ma, X. L.; Sun, Q.; Jiang, Z. Y. *J. Membr. Sci.* **2007**, *294*, 68.
16. Castro, A. J. U. S. Pat. 4,247,498, **1981**.
17. Van de Witte, P.; Dijkstra, P. J.; Van den Berg, J. W. A.; Feijen, J. *J. Membr. Sci.* **1996**, *117*, 1.
18. Yang, J.; Li, D. W.; Lin,Y. K.; Wang, X. L.; Tian, F.; Wang, Z. *J. Appl. Polym. Sci.* **2008**, *110*, 341.
19. Lin, Y. K.; Tang, Y. H.; Ma, H. Y.; Yang, J.; Tian, Y.; Ma, W. Z.; Wang, X. L. *J. Appl. Polym. Sci.* **2009**, *114*, 1523.
20. Hirami, K.; Ohmukai, Y.; Maruyama, T.; Matsuyama, H. *Desalin. Water Treat.* **2010**, *17*, 262.
21. Liang, H. Q.; Wu, Q. Y.; Wan, L. S.; Huang, X. J.; Xu, Z. K. *J. Membr. Sci.* **2013**, *446*, 482.
22. Matsuyama, H.; Ohga, K.; Maki, T.; Tearamoto, M.; Nakatsuka, S. *J. Appl. Polym. Sci.* **2003**, *89*, 3951.
23. Dean, J. A. Lange's Handbook of Chemistry Version 16th; McGraw-Hill: New York, **1999**.
24. Xiao, Y.; Liu, X. D.; Wang, D. X.; Lin, Y. K.; Han, Y. P.; Wang, X. L. *Desalination* **2013**, *311*, 16.
25. Matsuyama, H.; Takida, Y.; Maki, T.; Teramoto, M. *Polymer* **2002**, *43*, 5243.
26. Shibutani, T.; Kitaura, T.; Ohmukai, Y.; Maruyama, T.; Nakatsuka, S.; Watabe, T.; Matsuyama, H. *J. Membr. Sci.* **2011**, *376*, 102.
27. Flory, P. J. Priciples of Polymer Chemistry; Cornell University Press: New York, **1953**.
28. Arthanareeswaran, G.; Kumar, S. A. *J. Porous Mater.* **2010**, *17*, 515.
29. Altena, F. W.; Schroder, J. S.; Vandehuls, R.; Smolders, C. A. *J. Polym. Sci. Polym. Phys.* **1986**, *24*, 1725.
30. Peng, N.; Widjojo, N.; Sukitpaneenit, P.; Teoh, M. M.; Lipscomb, G. G.; Chung, T. S.; Lai, J. Y. *Prog. Polym. Sci.* **2012**, *37*, 1401.
31. Reuvers, J.; Altena, F. W.; Smolders, C. A. *J. Polym. Sci. Poyml. Phys.* **1986**, *24*, 793.
32. Tanaka, H. *J. Chem. Phys.* **1996**, *105*, 10099.
33. Li, Y. C.; Shi, R. P.; Wang, C. P.; Liu, X. J.; Wang, Y. *Mater. Sci. Eng.* **2012**, *20*, 14.
34. Tsai, F. J.; Torkelson, J. M. *Macromolecules* **1990**, *23*, 775.
35. McGuire, K. S.; Laxminarayan, A.; Lloyd, D. R. *Polymer* **1995**, *36*, 4951.
36. Barton, B. F.; McHugh, A. J. *J. Membr. Sci.* **2000**, *166*, 119.
37. Barton, B. F.; Graham, P. D.; McHugh, A. *J. Macromolecules* **1998**, *31*, 1672.
38. Arthanareeswaran, G.; Thanikaivelan, P. *Sep. Purif. Technol.* **2010**, *74*, 230.
39. Maheswari, P.; Mohan, D. *High Perform. Polym.* **2013**, *25*, 641.
40. Arthanareeswaran, G.; Sriyamuna Devi, T. K.; Raajenthiren, M. *Sep. Purif. Technol.* **2008**, *64*, 38.
41. Sukitpaneenit, P.; Chung, T. S. *J. Membr. Sci.* **2009**, *340*, 192.
42. Chung, T. S.; Teoh, S. K.; Hu, X. *J. Membr. Sci.* **1997**, *133*, 161.